Multiple Confinements of Concrete Columns by Various Embedded Composite Grids

Y. GHERNOUTI*
LMMC, Laboratory of Minerals Materials and Composites
University of Boumerdes, Algeria

K. AIT TAHAR
LaMoMS, Laboratory of the Department of Civil Engineering
University of Tizi Ouzou, Algeria

ABSTRACT: This study exhibits the experimental results of axial compression tests on concrete cylinders, circumferentially confined by the set-up of the composite grids arranged inside the cylinder, according to several combinations of circumscribed grids. The main aim is to verify the applicability of this method and then to quantify the contribution to strength improvement due to confinement as well as its influence on the rupture mode under axial compression. The test results of loading carried out on cylindrical concrete specimens, confined by alveolus composite grids arranged inside the section, show that it is possible to substantially increase the ductility of the columns, and in certain cases, their strength. It is also noted that the rupture of confined concrete is highly influenced by the presence of the grids depending on the configuration and the shape of the cells (rhombus or hexagonal) constituting the composite grid. The experimental results are compared with the theoretical model data.

KEY WORDS: concrete, confinement, composite grid, hybrid, axial compression, rupture.

INTRODUCTION

THE APPLICATIONS OF composite materials in civil engineering structures is in increasing development because of their interesting characteristics and their contribution in terms of rigidity, strength, and deformability, modifying completely or partially the concrete behavior, especially in tension where concrete exhibits a low strength.

The recent applications make it possible to locate, among the wide range of potential uses of these new materials, the technique of confinement of concrete columns by using jackets of composite materials. Several methods and techniques are proposed by various authors [1–3].

These various techniques put forward a confinement of the external wall according to various processes, by joining of sheets, armed spirals, and steel wires [4,5].

The lateral confinement of concrete columns makes it possible to increase the compressive strength and the ultimate strain by rolling up a composite material jacket

*Author to whom correspondence should be addressed. E-mail: y_ghernouti@yahoo.fr
Figures 1–8 and 10 appear in color online: http://jrp.sagepub.com

0731-6844/09/12 1495–13 $10.00/0 DOI: 10.1177/0731684408092367

Los Angeles, London, New Delhi and Singapore

on the concrete surface [6,7,8,15]. This reduces the formation and the opening of cracks in the concrete and retains transverse strain due to internal cracking. In this type of element the concrete resists the compression whereas the composite resists tension and shearing loads. This technique seems to be an interesting alternative to the traditional approaches.

Mirmiran et al. [9] manufactured round and square FRP tubes that were filled with concrete and then tested in compression. The round tubes increased the peak axial stress by as much as 2.5 times the peak axial stress of unconfined concrete and reached axial strains 12 times higher than the axial strain at peak stress of unconfined concrete.

Shahawy et al. [10] tested standard concrete cylinders wrapped with carbon fiber fabrics in an epoxy matrix. The results varied depending on the number of carbon layers applied. For an unconfined concrete strength of 41.4 MPa the confined strength of cylinders was increased to 70 MPa for the one layer wrap and 110 MPa for the four layer wrap. The ultimate strain for the one layer wrap was 0.007 and for the four layer wraps 0.016.

Xiao and Wu [6,11], Lam and Teng [12], Li et al. [13], Harries and Kharel [14], and Li and Hadi [15] tested concrete cylinders wrapped with FRP composites. The strength of FRP confined concrete was increased compared to the unconfined concrete, between 1 and 420% depending on the type and amount of FRP composite.

This study presents the preliminary results of an experimental study on the behavior of confined concrete columns, with different composite grids. This is a new technique that requires investigation of the level of confinement provided by the grids.

To further investigate this fact, an experimental program was carried out consisting of the study of cylinders 160×320 mm circumferentially confined according to several configurations by alveolus composite grids arranged inside the cylinders. All specimens were tested under axial compression.

EXPERIMENTAL PROCEDURE

The experimental program of this study includes 15 series of tests on cylindrical columns confined by alveolus composite grids under axial compression.

The objects of these tests are, on the one hand, to quantify the contribution in resistance conferred on the specimen by the composite grids, and on the other hand to estimate the contribution in ductility according to the following arrangements: confinement by only one grid arranged outside (three series); at the interior (three series); simultaneous confinement by two circumscribed grids one inside the other of the same nature (three series); and hybrid (six series). The influence of the configuration is observed on the rupture mode and on the levels, as well as on the longitudinal strain at the cylinder failures.

Materials Used

All the cylinders of dimensions 160×320 mm were carried out with only one composition of aggregates, comprising a crushed coarse sand supplied by the TIZI quarry (Mascara, Algeria) and two types of gravel (3/8) and (8/15). Cement of the type CEM II 32.5 was supplied by the cement factory of CHLEF (Algeria) with resistance 43 MPa.

The maximum coarse aggregate size was restricted to 15 mm, so that the aggregate particles could easily pass between the cells of the grids. Water/cement and aggregate/cement were used with ratios of 0.41 and 4.41, respectively. The average compressive strength of the concrete was approximately 25 MPa.

Raw Composite Material

In this study, three types of material were chosen by considering their cheapness and availability: metallic grids, polypropylene grids with rhombus cells, and metallic grids with hexagonal cells. Various alternatives of these grids are presented in Figure 1 and the geomechanical properties are given in Tables 1 and 2.

Confinement Alternatives

In order to evaluate the efficiency of the confinement provided by composite grid sheets to increase the concrete strength and ductility, 15 alternatives of confinement by multiple composite grids in the concrete matrix were elaborated. The configurations are indicated in Table 3. Figure 2 illustrates examples of the composite grid arrangement in the concrete matrix.

The integration of only one grid in the matrix concrete allowed confined concrete to confer a greater reserve of resistance and ductility.

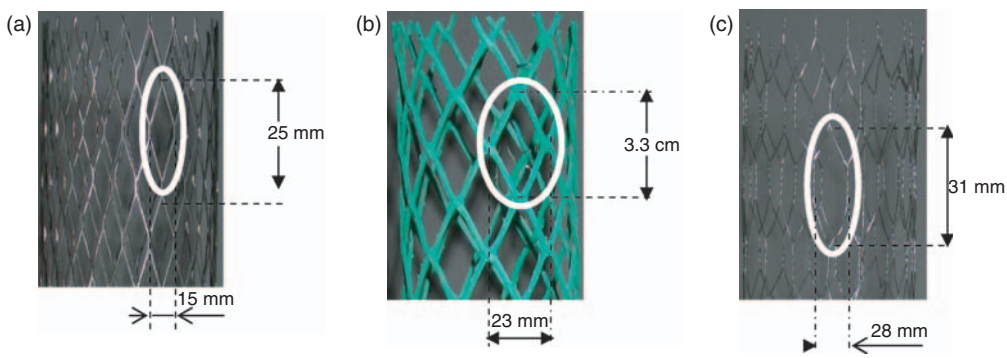

Figure 1. *Shapes of used grids: (a) metallic grid with rhombus cells (GMR), (b) polypropylene grid with rhombus cells (GPP), (c) metallic grid with hexagonal cells (GMH).*

Table 1. Geometrical properties of the grids.

	Metallic grid with rhombus cells (GMR)	Polypropylene grid (GPP)	Metallic grid with hexagonal cells (GMH)
Mass (g)/m^2	900	500	250
Number of (mesh/m^2)	1952	936	1269
Diameter (mm)	1	3	0.55

Table 2. Mechanical properties of the grids.

	Metallic grid with rhombus cells (GMR)	Polypropylene grid (GPP)	Metallic grid with hexagonal cells (GMH)
Breaking load (kN)	112	88	159.1
Breaking stress (MPa)	471.4	4.27	167.4
Lengthening at rupture (%)	5.72	117.17	7.37

Table 3. Type of configuration and grids used.

Type of configuration	Material used
One grid	
Exterior	GMR GPP GMH
Interior	GMR GPP GMH
Two identical grids	GMR + GMR GPP + GPP GMH + GMH
Hybrid	GMR + GMH GMH + GMR GMR + GPP GPP + GMR GMH + GPP GPP + GMH

Figure 2. *Examples of grid arrangements: (a) exterior grid, (b) interior grid, (c) hybrid grid.*

Figure 3. *Measurement devices and loading of the specimens.*

The integration of two grids made it possible to produce a double confinement. Indeed, the central concrete element underwent the effect of the two grids, whereas the second element was only confined by one grid. Therefore the concrete which was confined between the two grids will behave as a ring subjected to a compression radial stress due to the rigidity difference between the concrete and the grids. For this purpose, the grids played different roles: the first role consisted in confining the concrete, which provided great strength, the second role consisted in exerting a radial pre-stressing of compression on the ring, and finally, during crushing, the concrete hard cores remained imprisoned inside the grids, which allowed us to extend the time for total destruction of the element.

Specimen Preparation

Different cylinders were cast. The circular columns were 160 mm in diameter with 320 mm side length. The various composite grids were carefully arranged and cast out inside the cylindrical molds while the remaining three cylinders were cast without reinforcement.

The filling was carried out in three phases. For each phase, a vibration of the mold was carried out using a mobile stripe for 20 s. For each series, three specimens were made by using the same composition. After demolding, the specimens were deposited in a water vat for 28 days.

Loading Procedure and Acquisition

The specimens were placed one at a time in a 1500 Kn ELE TEST hydraulic machine, and subjected to an increasingly compressive axial load, under a constant rate of 0.20 MPa/s, until failure. At load intervals of 50 Kn, with displacement control, the lower tray is fixed and the higher support is mobile. To ensure parallelism and flatness of the faces of support, an operation of surfacing is first applied to the two ends of the cylinders. A quasi static rate of loading is applied with a speed of 10 kN/s.

The force and the axial strain are measured at close intervals at the medium of the two opposite sides and on the two opposite corners, approximately at mid-height column.

RESULTS AND DISCUSSION

The obtained axial stress–longitudinal strain curves for some of the confined concrete columns are shown in Figures 4–7. In these figures, it can be seen clearly that both the stress and strain at failure for the confined columns were higher than those for the unconfined ones, and the highest values were obtained for hybrid confined circular columns with polypropylene grid and metallic hexagonal cells.

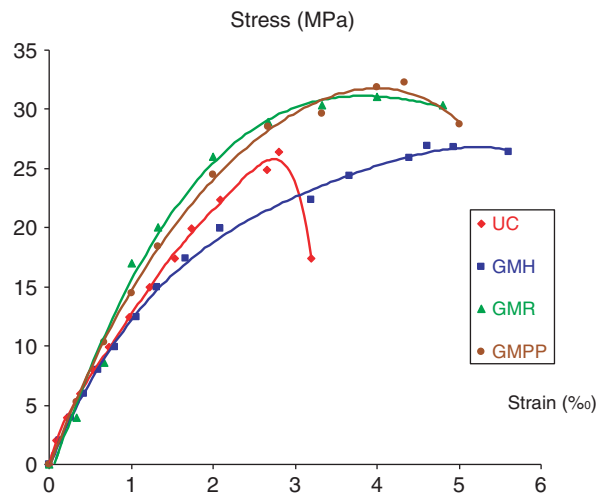

Figure 4. *Stress–strain curves for reference concrete and concrete with one exterior grid.*

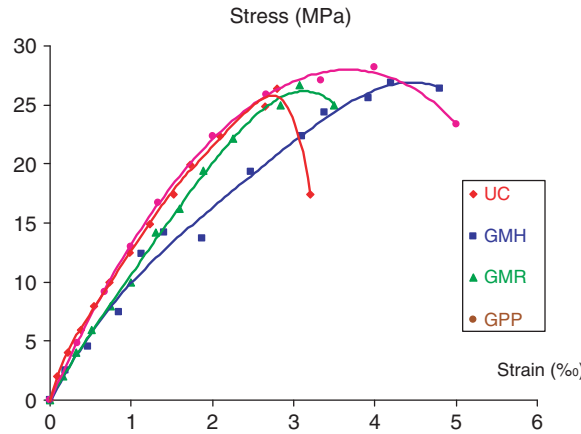

Figure 5. *Stress–strain curves for reference concrete and concrete with one interior grid.*

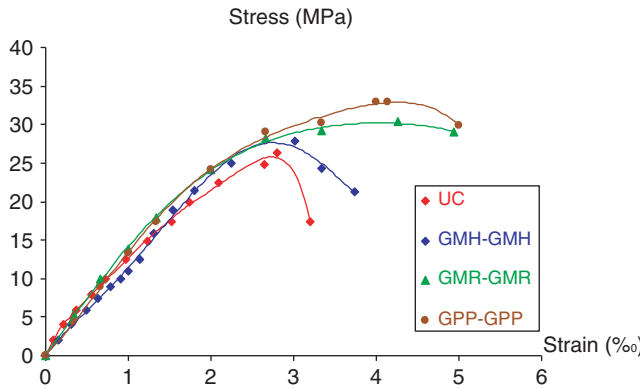

Figure 6. *Stress–strain curves for reference concrete and concrete with two identical grids.*

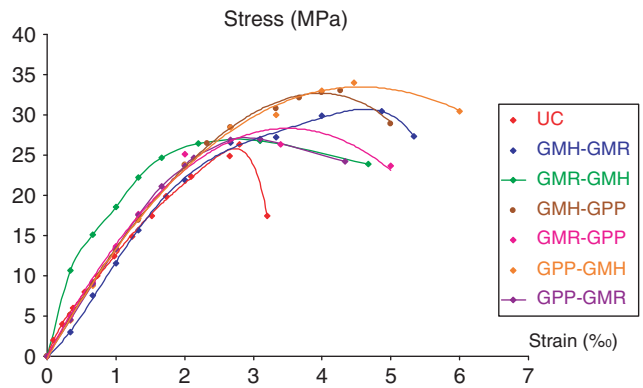

Figure 7. *Stress–strain curves of the concrete with hybrid grids.*

Table 4. Compressive strength and strain average values for the tested columns.

Column		Unconfined concrete			Confined concrete				
		f_{c0} (MPa)	ε_{co} (‰)	ε_u (‰)	f_{cc} (MPq)	ε_{cc} (‰)	f_{cc}/f_{c0}	$\varepsilon_{cc}/\varepsilon_{co}$	ε_{cu} (‰)
Unconfined concrete 'UC'		26.36	2.8	3.2	–	–	–	–	–
Exterior grid	GMH				26.85	4.6	1.02	1.6	5.6
	GMR				31.08	4.0	1.18	1.4	4.8
	GMPP				32.27	4.3	1.22	1.5	5.0
Interior grid	GMH				26.85	4,2	1.02	1.5	4.8
	GMR				26.68	3.1	1.01	1.1	3.5
	GPP				28.20	4.0	1.07	1.4	5.0
GMH-GMH					27.89	3.0	1.06	1.1	3.7
GMR-GMR					30.34	4.3	1.15	1.5	4.9
GPP-GPP					32.97	4.1	1.25	1.5	5.0
GMH-GMR					30.43	4.8	1.15	1.7	5.3
GMR-GMH					26.76	3.1	1.02	1.1	4.6
GMH-GPP					33.02	4.3	1.25	1.5	5.0
GMR-GPP					26.36	3.4	1.00	1.2	5.0
GPP-GMH					34.02	4.5	1.29	1.6	6.0
GPP-GMR					27.01	3.1	1.02	1.1	4.3

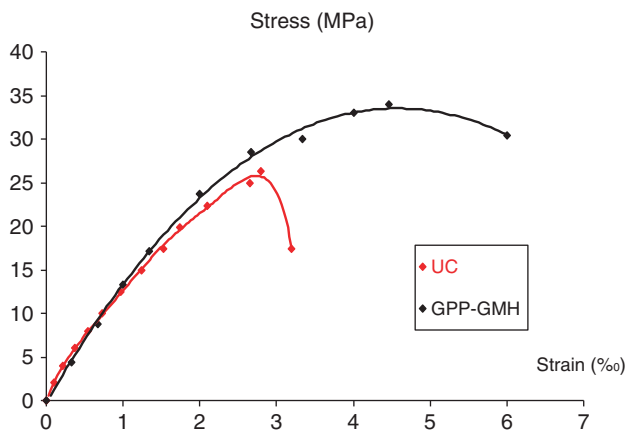

Figure 8. *Reference concrete left and confined concrete right BC (PP-MH) (better alternative).*

From Table 4, it can be seen that the increase in strength and ductility varied according to the type of composite grid and its arrangement. For all the specimens, ratios f_{cc}/f_{c0} and $\varepsilon_{cc}/\varepsilon_{c0}$ are always significant, presenting values superior to one.

For confined columns, the average increase in strength and ductility were of the order of 29 and 87.5%, respectively. It is clear from Table 4 that this increase provided by confinement is very sensitive to the cross-section geometry of the composite grid and the hybrid configuration that was used.

All the test results of an axial compression are illustrated in Figures 4–8.

For the case of the columns confined by only one grid arranged inside the columns (Figure 2(b)), there was a weak increase in resistance compared to the unconfined concrete,

Figure 9. *Mode of rupture of the reference concrete and confined concrete.*

probably due to the rigidity of the grid composites that makes all the load of compression concentrate on the layer of coating causing the rupture of the test-tube at this level. While for columns confined with a grid disposed outside (Figure 2(a)), a remarkable improvement of strength and ductility of about 22 and 56%, respectively, is present, the layer of coating of the grids is very fine (few millimetres) which causes fast corrosion of these grids.

For the columns that are confined by two identical grids, we observe in Figure 6 clear improvement of ductility and in most cases an increase in resistance at various degrees according to the grid type. As indicated, the concrete confined by polypropylene grids shows a (average) strength of 33 MPa, and thus an increase of about 25%, and an ultimate strain of 5%; so an improvement of 56.25%. This is due to the effect of compression by confinement grids, which prevents the beginning and thus the propagation of cracks in the concrete.

For concrete columns with hybrid confinement, the contribution in strength of confinement is assessed according to the type of grids and their arrangement [16]. Indeed, by modifying these two parameters, an effect is directly observed on the mode of rupture which is seen through both the strength level and the ultimate strain (Figure 9). In this image, we observe that the concrete hard cores remain imprisoned inside the grids and the cores of the specimens remain unbroken, which leads to progressive rupture of the element contrary to the reference concrete, presenting a brutal rupture.

In general, the various obtained results show clearly that strength in axial compression of the confined columns increases compared to the unconfined columns. The mechanical output is influenced, in a more or less pronounced way, according to the type of grids used. As an indication, the compressive strength of the columns confined with polypropylene grids and metallic grids of hexagonal form (Figure 8) is greater by 29% than for unconfined columns. The maximum gain of ductility in compression is 87.5% compared to unconfined columns.

The hybridization of the grids provided to the concrete columns give better performance concerning the strengths and the ductility [16], probably due to the conjugation of the properties of each type of grid. Indeed, the polypropylene grids improve deformability whereas the metallic grids improve resistance.

CALIBRATION OF THE CONFINEMENT PARAMETERS

The theoretical study of the elements reinforced by composite materials shows that the mechanical behavior of the compressed concrete is linear elastic followed by a nonlinear curve. In the literature, several analytical models are proposed to give the ultimate strength of confined concrete f_c and the corresponding ultimate strain ε_c [17–21].

As summary of some of the expressions found in the literature, for estimating the confined concrete strength and the axial strain at failure, is presented in Table 5.

Confinement can improve both the compressive strength and ductility of concrete.

Most models have been refined using data from concrete that is confined by FRP composite materials where the amount and properties produce such behavior.

Assuming that the confined concrete is in a triaxial stress state, the increase in strength provided by the confinement is reflected in the maximum stress (f_{cc}) for a cylindrical specimen, which is defined as (Mander et al. [16]):

$$f_{cc} = f_{co} + k_1 f_{ru} \tag{1}$$

where k_1 is the confinement effectiveness coefficient and f_{ru} is the confinement strength. The confinement effectiveness coefficient for concrete confined by steel is usually between 2.8 and 4.1. Campione and Miraglia [28] found that the above values overestimate the confinement effectiveness coefficient for concrete wrapped with FRP. They also found that the confinement effectiveness coefficient for FRP wrapped concrete was 2. For the purpose of this study the confinement effectiveness coefficient was taken as 2. The axial strain of CFRP grid confined concrete at the peak stress (ε_{cc}) was determined in a similar manner as unconfined concrete using the expression (MacGregor [29]):

$$\varepsilon_{cc} = 1.8.\frac{f_{cc}}{E_c}. \tag{2}$$

Equations (1) and (2) were combined with the modified Hognestad stress–strain equation as follows [30]:

$$\text{AB} - f_c = f_{cc}\left[\frac{2\varepsilon_c}{\varepsilon_{cc}} - \left(\frac{\varepsilon_c}{\varepsilon_{cc}}\right)^2\right] \tag{3a}$$

$$\text{BC} - f_c = f_{cc}[1 - D_c(\varepsilon_c - \varepsilon_{cc})] \tag{3b}$$

where ε_c is the concrete strain, ε_{cc} is the strain at peak stress of unconfined concrete, and ε_{cu} is the ultimate strain.

The modified Hognestad equations model the ascending branch (AB) with a parabolic relationship and the descending branch BC with a linearly descending curve. The equation for region BC is based on the deterioration constant (D_C) that controls the slope of the line Figure 10.

To calibrate the parameters, we applied the Hognested model. Equations (3a) and (3b) have been compared with the experimental results of the concrete confined by integrated embedded grids. Confrontation of the stress–strain experimental and theoretical curves is given in Figure 11.

Table 5. Expressions for the strength of confined concrete and maximum axial deformation.

Author	Type of confinement	Strength f_{cc}	Ultimate axial strain ε_{cc}
Fardis & Khalili [22]	GFRP encased concrete	$f_{c0}\left[1+2.05\left(\frac{f_1}{f_{c0}}\right)\right]$	$0.002\left[1+0.5\left(\frac{E_f \cdot t_f}{D \cdot f_{c0}}\right)\right]$
Karbahari & Eckel [23]	FRP encased concrete	$f_{c0}\left[1+2.1\left(\frac{f_1}{f_{c0}}\right)^{0.87}\right]$	$0.002\left[1+5\left(\frac{2t_f \cdot f_f}{D \cdot f_{c0}}\right)\right]$
Mirmiran & Shahawy [24]*	GFRP encased concrete	$f_{c0}+4.269f_l^{0.587}$	
Samaan et al. [25]*	GFRP encased concrete	$f_{c0}+6.0f_l^{0.7}$	$\frac{f_{cc}-0.872f_{c0}-0.371f_f-6.258}{245.61f_{c0}^{0.2}+1.3456(E_f t_f/D)}$
Toutanji [26]	CFRP and GFRP wrapped concrete	$f_{c0}\left[1+3.5\left(\frac{f_1}{f_{c0}}\right)^{0.85}\right]$	$\varepsilon_{c0}\left[1+(310.57\varepsilon_f+1.9)\left(\frac{f_{cc}}{f_{c0}}-1\right)\right]$
Spoelstra & Monti [27]	CFRP and GFRP wrapped and encased concrete	$f_{c0}\left[0.2+3\left(\frac{f_1}{f_{c0}}\right)^{0.5}\right]$	$\varepsilon_{c0}\left[2+1.25\frac{E_c}{f_{c0}}\varepsilon_f\sqrt{\frac{f_l}{f_{c0}}}\right]$

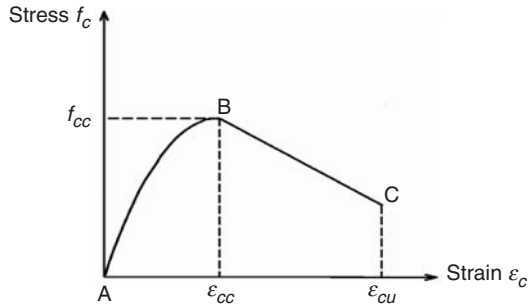

Figure 10. *Modified stress–strain curve of Hognestad [31]*

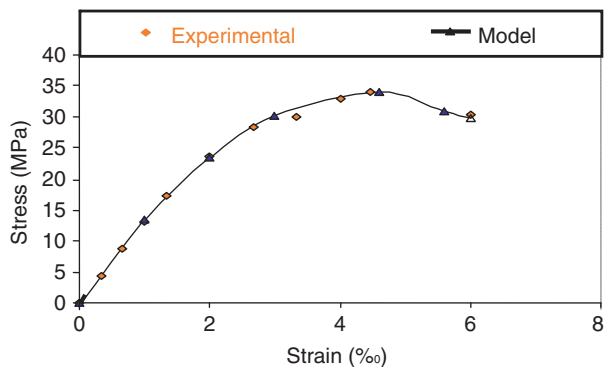

Figure 11. *Confrontation of the stress–strain experimental curves and theoretical.*

The modified Hognestad curve matches well with the experimental curve; the predicted value is 0.6% of the concrete confined by integrated embedded grids compared with theoretical values obtained by application of the modified Hognestad model. We can see a good agreement of the values.

CONCLUSIONS

The experimental study that we have presented in this article is of a promising revelation of the performance of the proposed process with multiple confinements with hybrid grids.

Concrete cylinders with embedded composite grids were tested in compression to failure to determine the post-peak behavior and ability of the grid to provide confinement to the concrete.

The conjugation of the mechanical performances of the polypropylene and metallic grids makes it possible to fulfill the requirements of confinement. Indeed, the grids make it possible to confine concrete and at the time of failure keep its imprisoned hard cores inside. The choice of grids with mesh of size higher than the grains is justified by the concern for ensuring the continuity of the concrete. Thus, the modes of rupture are not a function of the interface obtained by the coupling of shearing and of the normal stress, or a rupture in traction of the concrete layer located between composite material and the matrix concrete.

Finally, the size of the mesh of the grids and their form (rhombus and hexagonal), the nature of the grids, their strength f_f, and their modulus of elasticity, are parameters that are necessary to study for an optimization of the contribution of the composite envelopes (value of ρ_f) and their influence on the degree of confinement and ultimate strength.

REFERENCES

1. Ahmad, S. H. and Shah, S. P. (1982). Stress–Strain Curves of Concrete Confined by Spiral Reinforcement, *ACI Journal*, **79**: 484–490.
2. EL-Dash, K. M. and Ahmad, S. H. (1995). A Model for Stress-Strain Relationship of Spirally Confinement Normal and Height Strength Concrete Columns, *Magazine of Concrete Research*, **47**: 177–184.
3. Mander, J. B., Priestley, M. J. and Park, K. (1988). Observed Stress-Strain Behavior of Confined Concrete, *Journal of Structural Engineering*, ASCE, **114**(8): 1827–1849.
4. Leung, H. Y. (2000). Aramid Spirals to Confine Concrete in Compression, PhD Thesis, p. 200, University of Cambridge.
5. Kim, J.-K. and Chan-Kyu Park (1999). The Behavior of Concrete Columns with Interlocking Spirals, *Engineering Structure*, **21**: 945–953.
6. Xiao, Y. and Wu, H. (2003). A Compressive Behavior of Concrete Confined by Various Types of FRP Composite Jackets, *Journal of Reinforced Plastics and Composites*, **22**(13): 1187–1201.
7. Berthet, J. F., Ferrier, E. and Hamelin, P. (2005). Compressive Behavior of Concrete Externally Confined by Composite Jackets. Part A: Experimental Study, *Constriction and Building Materials*, **19**: 223–232.
8. Bentayeb, F., Ait Tahar K. and Chateauneuf, A. (2008). New Technique for Reinforcement of Concrete Columns Confined by Embedded Composite Grid, *Construction and Building Materials*, **22**(8): 1624–1633.
9. Mirmiran, A., Shahawy, M., Samaan, M., El Echary, H., Mastrapa, J. C. and Pico, O. (1998). Effect of Column Parameters on FRP-Confined Concrete, *Journal of Composites for Construction*, **2**(4): 175–185.
10. Shahawy, M., Mirmiran, A. and Beitelman, T. (2000). Tests and Modeling of Carbon-Wrapped Concrete Columns, *Composites Part B: Engineering*, **31**: 471–480.
11. Xiao, Y. and Wu, H. (2000). Compressive Behavior of Confined Concrete by Carbon Fiber Composite Jackets, *Journal of Materials in Civil Engineering*, **12**(2): 139–146.
12. Lam, L. and Teng, J. G. (2004). Ultimate Condition of Fiber Reinforced Polymer-Confined Concrete, *Journal of Composites for Construction*, **8**(6): 539–548.
13. Li, Y., Lin, C. and Sung, Y. (2002). Compressive Behavior of Concrete Confined by Various Types of FRP Composite Jackets, *Mechanics of Materials*, **35**: 603–619.
14. Harries, K. A. and Kharel, G. (2002). Experimental Investigation of the Behavior of Variably Confined Concrete, *Cement and Concrete Research*, **33**(6): 873–880.
15. Li, Y. and Hadi, M. N. S. (2003). Behaviour of Externally Confined High-Strength Concrete Columns under Eccentric Loading, *Composites for Construction*, **62**(2): 145–153.
16. Guoqiang Li. (2007). Experimental Study of Hybrid Composite Cylinders, *Composite Structures*, **78**: 170–181.
17. Berthet, J. F., Ferrier, E. and Hamelin, P. (2006). Compressive Behavior of Concrete Externally Confined by Composite Jackets. Part B: Modeling. *Constriction and Building Materials*, **20**: 338–347.
18. Baris Binici. (2005). An Analytical Model for Stress-Strain Behavior of Confined Concrete, *Journal of Engineering Structure*, **27**: 1040–1051.
19. Mander, J. B., Priestley, M. J. and Park, K. (1988). Theoretical Stress-Strain Model for Confined Concrete, *Journal of Structural Engineering*, ASCE, **114**(8): 1804–1826.
20. Marwan, N. Y., Maria, Q. F. and Ayman, S. M. (2007). Stress-Strain Model for Concrete Confined by FRP Composites, *Composites: Part B: Engineering*, **38**: 614–628.
21. Mohamed, H. Harajli. (2006). Axial Stress-Strain Relationship for FRP Confined Circular and Rectangular Concrete Columns, *Cement and Concrete Composites*, **28**: 338–948.
22. Fardis, M. N. and Khalili, H. (1981). Concrete Encased in Fiberglass-Reinforced Plastic, *ACI Journal*, **78**(6): 440–446.
23. Karbahari, V. M. and Eckel, D. A. (1993). Strengthening of Concrete Column Stubs Through Resin Infused Composite Wraps, *Journal of Thermoplastic Composite Materials*, **6**(2): 92–107.
24. Mirmiran, A. and Shahawy, M. (1997). Behavior of Concrete Columns Confined by Fiber Composites, *Journal of Structural Engineering*, ACSE, **123**(5): 583–590.

25. Samaan, M., Mirmiran, A. and Shahawy, M. (1998). Model of Concrete Confined by Fiber Composites, *Journal of Structural Engineering*, ACSE, **124**(9): 1025–1031.
26. Toutanji, H. A. (1999). Stress-Strain Characteristics of Concrete Columns Externally Confined with Advanced Fiber Composite Sheets, *Materials Journal*, ACI, **96**(3): 397–404.
27. Spoelstra, M. R. and Monti, G. (1999). FRP-Confined Concrete Model, *Journal of Composites for Construction*, ASCE, **3**(3): 143–150.
28. Campione, G. and Miraglia, N. (2003). Strength and Strain Capacities of Concrete Compression Members Reinforced with FRP, *Cement and Concrete Composites*, **25**(1): 31–41.
29. MacGregor, J. G. (1997). Chapter 3: Materials, *Reinforced Concrete: Mechanics and Design*, **3rd edn**, pp. 35–81, Prentice Hall, New Jersey.
30. Michael, A. P., Hamilton III, H. R. and Ansley, M. H. (2005). Concrete Confined using Carbon Fiber Reinforced Polymer Grid, *International Symposium on Fiber Reinforced Polymer Reinforcement for Reinforced Concrete Structures* "*66FRPRCS-7*", pp. 991–1009.
31. Park, R. and Paulay, T. (1975). Chapter 6: Ultimate Deformation and Ductility of Members with Flexure, *Reinforced Concrete Structure*, pp. 195–269, John Wiley and Sons, New York.